Mast cell- and dendritic cell-derived exosomes display a specific lipid composition and an unusual membrane organization

Karine LAULAGNIER*, Claude MOTTA†, Safouane HAMDI*, Sébastien ROY*, Florence FAUVELLE‡, Jean-François PAGEAUX§, Toshihide KOBAYASHI§‖, Jean-Pierre SALLES*, Bertrand PERRET*, Christian BONNEROT¶ and Michel RECORD*[1]

*INSERM U563, Département "Lipoprotéines et Médiateurs Lipidiques", CPTP, Place du Dr Baylac, Hôpital Purpan, 31059 Toulouse Cedex 03, France, †CHU Pontchaillou, Laboratoire de Biochimie, 2 rue Henri Le Guilloux, 35000 Rennes, France, ‡Centre de Recherche du service de Santé des Armées (CRSSA), Avenue du Grésivaudan, 38700 La Tronche, France, §INSERM U585 "Physiopathologie des lipides et des membranes", INSA, 20 Avenue Albert Einstein, 69621 Villeurbanne, France, ‖Riken Institute, Hirosawa, Wako, Saitama 351-0918, Japan, and ¶INSERM U520 "Biologie Cellulaire de l'Immunité anti-tumorale", Institut Curie, 26 rue d'Ulm, 75248 Paris, France

Exosomes are small vesicles secreted from multivesicular bodies, which are able to stimulate the immune system leading to tumour cell eradication. We have analysed lipids of exosomes secreted either upon stimulation from rat mast cells (RBL-2H3 cells), or constitutively from human dendritic cells. As compared with parent cells, exosomes displayed an enrichment in sphingomyelin, but not in cholesterol. Phosphatidylcholine content was decreased, but an enrichment was noted in disaturated molecular species as in phosphatidylethanolamines. Lyso(bis)phosphatidic acid was not enriched in exosomes as compared with cells. Fluorescence anisotropy demonstrated an increase in exosome-membrane rigidity from pH 5 to 7, suggesting their membrane reorganization between the acidic multivesicular body compartment and the neutral outer cell medium. NMR analysis established a bilayer organization of exosome membrane, and ESR studies using 16-doxyl stearic acid demonstrated a higher flip-flop of lipids between the two leaflets as compared with plasma membrane. In addition, the exosome membrane exhibited no asymmetrical distribution of phosphatidylethanolamines. Therefore exosome membrane displays a similar content of the major phospholipids and cholesterol, and is organized as a lipid bilayer with a random distribution of phosphatidylethanolamines. In addition, we observed tight lipid packing at neutral pH and a rapid flip-flop between the two leaflets of exosome membranes. These parameters could be used as a hallmark of exosomes.

Key words: exosome, lipid domain, lipid bilayer, lipid flip-flop, membrane asymmetry, membrane rigidity.

INTRODUCTION

Previous studies have shown that cell communication might not be limited to soluble agonists, but that various types of vesicles also participate in the process [1]. In this respect, exosomes appear as a new category of such vesicles, able to stimulate the immune system *in vivo*. Zitvogel et al. [2] have shown that exosomes, secreted by DCs (dendritic cells) previously sensitized to tumoral antigenic peptides, exhibit anti-tumoral properties against P815 mouse mastocytoma. Considering these observations, clinical trials have been undertaken with human DC-derived exosomes used against human melanoma and lung cancers [3].

Concerning exosome origin, several groups have observed, by electron microscopy, that late endosomes, often referred to as MVBs (multivesicular bodies), contain small vesicles. When the MVB compartment fuses with the plasma membrane, whether constitutively or under stimulation, these vesicles of 60–90 nm, called exosomes, are released outside the cells [1]. Exosomes are secreted by various immunocompetent cells, and notably by APCs (antigen-presenting cells), such as DCs, B-cells and other occasional APCs, such as mast cells.

Different proteomic studies have shown an enrichment of functional MHC (major histocompatibility complex) class II and I molecules on exosomes [4,5], and of tetraspan family proteins such as CD63 or CD81 [6]. Such an enrichment could be important for the structure and function of exosomes, as suggested from studies on 'tetraspanin domains' [7].

According to electron-microscopy studies, exosomes are formed by inward budding of the limiting membrane of late endosomes [8]. In yeast and mammalian cells, the formation of such internal vesicles requires PtdIns(3,5)P_2 and PI3K (phosphoinositide 3-kinase) activity, and, more particularly, hVPS34 lipid kinase activity [9,10]. Other lipid molecules, such as LBPA [lyso(bis) phosphatidic acid, also called BMP, i.e. bis(monoacylglycerol) phosphate], have been shown to be enriched in internal membranes of MVBs [11]. Therefore lipid metabolism seems to be important in exosome biogenesis.

In vivo exosome anti-tumoral activities were observed using DC-derived exosomes [2]. Moreover, functional *in vitro* studies have shown that mast cells also secrete exosomes that play a key role in stimulating immunocompetent cell responses [12]. This study has shown that DCs are required as intermediates, since exosomes from the RBL-2H3 (rat basophile leukaemia) mast cell line are able to increase T-lymphocyte stimulation by a factor of log 2 in the presence of DCs with respect to exosomes alone [12]. In this respect, exosomes from mast cells, and not from B-lymphocytes or macrophages, can induce phenotypic and functional maturation of DCs [13]. In order to characterize precisely membranes of mast-cell- and DC-derived exosomes, we analysed the lipid composition and membrane organization of

Abbreviations used: AA, alkyl-acyl; AeA, alkenyl-acyl; APC, antigen-presenting cell; DA, diacyl; DAG, diacylglycerol; DC, dendritic cell; DHA, docosahexaenoic acid, DMEM, Dulbecco's modified Eagle's medium; DPH, 1,6-diphenyl-1,3,5-hexatriene; ER, endoplasmic reticulum; FAME, fatty acid methyl ester; FCS, foetal calf serum; LBPA, lyso(bis)phosphatidic acid; LDL, low-density lipoprotein; LPC, lysophosphatidylcholine; MHC, major histocompatibility complex; MVB, multivesicular body; PC, phosphatidylcholine; PE, phosphatidylethanolamine; PS, phosphatidylserine; PI, phosphatidylinositol; RBC, red blood cell; RBL-2H3, rat basophile leukaemia; SM, sphingomyelin; SUV, small unilamellar vesicle; TNBS, trinitrobenzene sulphonic acid.

[1] To whom correspondence should be addressed (e-mail record@cict.fr).

exosomes from these two myeloid cell types, using the RBL-2H3 mast cell line and human DC as secreting cells.

We observed that exosomes from these two cell types display a specific lipid composition and tight lipid packing, which increases between acidic and neutral pH. Also, the exosome membrane is characterized by a non-asymmetrical distribution of PE (phosphatidylethanolamine) and a rapid flip-flop of lipids between the two membrane leaflets. These characteristics distinguish exosomes from other types of cellular vesicles.

MATERIALS AND METHODS

Chemical reagents and antibodies

RPMI 1640, DMEM (Dulbecco's modified Eagle's medium), FCS (foetal calf serum), PBS, penicillin, streptomycin and L-glutamine were purchased from Gibco (Paisley, Scotland, U.K.). All solvents, alcohols and acids were from Merck Eurolab (VWR International, Fontenay s/Bois, France). All chemical reagents were from Sigma (St. Louis, MO, U.S.A.) except glycine (Eurobio, Paris, France). To prepare exoliposomes (liposomes with the same composition as natural exosomes) or control liposomes containing PC (phosphatidylcholine), lipids were purchased at Avanti Polar Lipids (Birmingham, AL, U.S.A.). A chloroformic solution of L-α-PC (egg PC, 100 mg/ml) and $MnCl_2$ were obtained from Sigma, as well as 16-doxyl stearic acid. Pure ^2H_2O was from Eurisotop (Saint-Aubin, France).

Cells

RBL-2H3 cells were provided by Dr Ulrich Blank (Pasteur Institute, Paris). They were grown in RPMI 1640 supplemented with 10 % (v/v) FCS, 4 mM L-glutamine, 140 units/ml penicillin and 140 μg/ml streptomycin, in a 5 % CO_2 humidified atmosphere at 37 °C. The cells were maintained either adherent or in suspension under slow constant agitation in 0.5 or 1 litre spinner bottles (VWR International). DCs and exosomes prepared from different batches of these cells were supplied by Anosys (Evry, France) and were of clinical grade [14].

Human RBCs (red blood cells) were purified from total blood harvested on anticoagulant from healthy donors. They were freshly prepared by recovering the lower phase after centrifugation of total blood at 4 °C for 10 min at 2000 ***g***.

Exosome preparation from RBL-2H3 cells

RBL-2H3 cells, grown in suspension, were degranulated for 20 min at 37 °C by stimulation with the calcium ionophore ionomycin (final concentration, 1 μM). Cell concentration was 10^8 cells in 5 ml of DMEM without FCS, to avoid contamination by microvesicles present in FCS. Exosomes were purified from the supernatants by differential centrifugations as reported previously [12,15]. Briefly, activated cells, debris and denser material were eliminated by consecutive centrifugations at 300 ***g*** for 5 min, 2000 ***g*** for 20 min at 4 °C and 10 000 ***g*** for 30 min at 4 °C. Finally, exosomes were isolated from the last supernatant by ultracentrifugation at 110 000 ***g*** at 4 °C for 70 min. The pellet was resuspended in PBS and centrifuged again at 110 000 ***g*** for 70 min at 4 °C. The final pellet, referred to as exosomes, was resuspended in PBS for analysis, and the protein concentration was determined by the Lowry method [16]. Usually, 300 μg of protein was obtained from exosomes prepared from 1×10^9 RBL-2H3 cells or DCs.

The purity of preparations was routinely checked by electron microscopy (by Dr D. Lankar and Dr C. Bonnerot, Institut Curie, Paris). Exosome pellets were resuspended and fixed in phosphate buffer containing 2 % (w/v) paraformaldehyde and then loaded on Formvar/carbon-coated electron-microscopy grids. The samples were contrasted in a mixture of methylcellulose and uranyl acetate and viewed with a CM120 Twin Philips electron microscope (Philips Electronic Instruments, Mahwah, NJ, U.S.A.).

Lipid extractions

Lipids from cells and exosomes were extracted by the Bligh and Dyer method, i.e. with chloroform/methanol/water (1:1:1, by vol.) in the presence of 1 % ethanoic acid in methanol [17]. The lower phase was collected, dried under nitrogen and diluted in chloroform/methanol (1:1, v/v) for storage or analysis. Total phospholipid content was measured by phosphorus quantification using the Fisk and Subarov method [18]. About 100 nmol of total phospholipids were recovered from exosomes prepared from 1×10^9 RBL-2H3 cells or DCs.

TLC separation of phospholipids

In order to separate the different classes of phospholipids, total lipid extracts of exosomes, RBL-2H3 cells and DCs were analysed by TLC on silica plates (0.25 mm thick; Merck) using the chromatographic system of Skipski et al. [19] as developing solvent (chloroform/methanol/ethanoic acid/water; 25:15:4:2, by vol.). The different classes of phospholipids were revealed by iodine vapours. This acidic system allowed the separation of PE ($R_f = 0.79$), PS (phosphatidylserine)/PI (phosphatidylinositol) ($R_f = 0.59$), PC ($R_f = 0.48$), SM (sphingomyelin) ($R_f = 0.27$) and LPC (lysophosphatidylcholine) ($R_f = 0.12$). When separation of PS and PI was required, the basic solvent system chloroform/methanol/40 % methylamine (65:22:4, by vol.) was used [20]. In order to evaluate the proportion of each class of phospholipids, the silica gel corresponding to each band was scraped off and free phosphate was then measured as above using the Fisk and Subarov method [18].

Analysis of phospholipid molecular species

Total lipid extracts of exosomes and RBL-2H3 cells were analysed by HPLC in three successive steps, in order to separate first the different classes of phospholipids, then the subclasses of PC and PE and finally the molecular species of these subclasses. For each of the three separation steps, lipid standards obtained from thymocytes were used [21]; other commercial standards allowed complete identification.

First, the various classes of phospholipids were separated by normal phase HPLC (Kontron Instruments) on a 250×4 mm Nucleosyl silica column with 7-μm-diameter spherical particles [22]. The injection solvent was hexane/isopropyl alcohol (3:2, by vol.) and the mobile phase acetonitrile/hexane/methanol/85 % phosphoric acid (918:30:30:17.5, by vol.). Separation was performed at a flow rate of 1.5 ml/min. Peak detection was monitored at $\lambda = 206$ nm using a UV detector from Kontron Instruments.

The classes of PC and PE were collected and converted into fluorescent derivatives. For this purpose, PC and PE were treated *in vitro* by phospholipase C, in the presence of diethyl ether, at 37 °C for 1 h. The DAGs (diacylglycerols) obtained were dissolved in acetonitrile, and derivatized by anthroyl chloride for 1 h at 70 °C, to obtain fluorescent DAGs (anthroyl-DAGs; [23]) which were extracted further by hexane/ether (1:1, by vol.), dried and dissolved in cyclohexane/ether (49:1, by vol.). Anthroyl-DAGs originating from PC and PE respectively were separated into three subclasses [AA (alkyl-acyl), DA (diacyl) and AeA (alkenyl-acyl)]

by normal phase HPLC on a 100 × 3 mm Equisorb silica column (Spherisorb®, Waters, St. Quentin en Yvelines, France) with 3-μm-diameter spherical particles [23]. The same solvents (cyclohexane/ether; 49:1, by vol.) were used as the mobile phase at a flow rate of 0.5 ml/min. Detection was monitored at $\lambda =$ 460 nm using an SFM 25 spectrophotometer (Kontron Instruments). The three types of anthroyl-DAGs corresponding to the three subclasses of PC or PE were collected and stored in acetonitrile/ether (1:1, by vol.).

In a third step, separation of molecular species was achieved with the technique and equipment reported by Thevenon et al. [21] and El Bawab et al. [24]. Briefly, reverse-phase HPLC was used, on a 250 × 4.6 mm Equisorb Octadecyl Silica 2 (ODS2) column with 5-μm-diameter spherical particles. The column was stabilized at 30 °C using a column heater. The mobile phase was acetonitrile/isopropyl alcohol (17:3, by vol.) at a flow rate of 1.5 ml/min [21]. The different fluorescent molecular species were detected at $\lambda = 460$ nm. Peaks were identified with respect to standard molecular species obtained from thymocytes or commercial sources as reported previously by Thevenon et al. [21]. Typical chromatograms of molecular species separation and peak identity confirmed by GLC are given in [21].

Measurement of LBPA

In order to purify and quantify LBPA in exosomes and RBL-2H3 cells, total lipid extracts were analysed according to the method described previously by Luquain et al. [20,25]. Briefly, LBPA was first separated from the other phospholipids by TLC on silica plates (0.25 mm thick; Merck) using the basic solvent system chloroform/methanol/40 % methylamine (65:22:4, by vol.) as the developing solvent. The phospholipids were revealed under UV light after spraying 2′,7′-dichlorofluorescein (0.05 % in methanol), and the band identified as LBPA ($R_f = 0.82$) was scraped off. The silica gel was then extracted three times using 3 ml of chloroform/methanol/water (5:5:1, by vol.), and water was added to the combined extracts to obtain proportions of 10:10:9 for chloroform/methanol/water. The lower phase was then harvested, dried under nitrogen and resuspended in dichloromethane. LBPA purity and quantity was then monitored at $\lambda = 205$ nm by HPLC on silica-NH_2 columns as described in [25]. This chromatographic system allowed LBPA to be resolved into three isomers that appeared after retention times of between 17 and 25 min.

Fatty-acid composition of LBPA was determined by GLC after *trans*-methylation as described previously [20]. FAME (fatty acid methyl ester) and dimethylacetal derivatives were analysed with a Hewlett Packard 5590 gas chromatograph. The capillary column was an SP2380 (0.32 mm × 30 m; Supelco, Bellefonte, PA, U.S.A.). The temperature was programmed from 145 to 225 °C at 1.2 °C/min. FAME and dimethylacetal derivatives were identified by comparison with the relative retention times of known standards. The percentage and mass of each fatty acid were computed using an internal standard as described previously [26].

In RBL-2H3 cells (see the Results section), as in other cell types (J.-F. Pageaux, unpublished work), LBPA isomers were essentially composed of poly- and mono-unsaturated fatty acids. Only cell incubation with exogenous DHA (docosahexaenoic acid) would modify LBPA fatty-acid content [20]. Such treatment was not performed in our experimental conditions. Thus we assumed that LBPA unsaturated-fatty-acid composition remained unchanged both in cells and exosomes and that UV detection of LBPA by HPLC allowed its quantitative measurement. At $\lambda = 205$ nm, 1980 units of integrated peak area corresponds to about 1 μg of LBPA.

Preparation of exoliposomes

Neutral lipids and phospholipids stored in chloroform/methanol (1:1, v/v) were mixed according to the composition of exosomes from RBL-2H3 cells reported in Figure 1(B). Solvent was evaporated and the lipid mixture (2 μmol) was resuspended in 2 ml of PBS and hydrated for 2 h at 55 °C with constant agitation. Exoliposomes were then prepared by extrusion with three passages through a 400-nm-diameter-pore-size membrane, followed by three passages through a membrane calibrated for 100 nm vesicles, using an extruder (Lipex Biomembranes, Vancouver, Canada) equipped with a 2 ml chamber. Liposomes made only with egg PC were prepared in a similar way.

Analysis of neutral lipids by GLC

Total lipid extracts were dried under nitrogen, and internal standards for cholesterol (stigmasterol; 3 μg) and DAGs (1,3-dimyristoylglycerol; 0.5 μg) were added. Lipids were dissolved in ethyl acetate for injection. Neutral lipids were resolved by GLC using a 5 m × 0.31 mm Hewlett Packard Ultra 1 capillary column [27]. The oven temperature was set up to follow a ramp from 205 °C to 345 °C at 6 °C/min, and hydrogen was used as carrier at a pressure of 50 kPa.

Analysis of membrane fluidity by fluorescence polarization [28]

The fluorescence polarization technique monitors anisotropy of a fluorescent membrane probe. The anisotropy is brought about by the restriction of movement of the probe in its lipid surroundings and hence gives information on lipid dynamics as the so-called fluidity/rigidity of membranes. The higher the fluorescence anisotropy value (r), the greater the rigidity of the membranes. The fluorescent hydrophobic probe DPH (1,6-diphenyl-1,3,5-hexatriene; $\lambda_{ex} = 350$ nm, $\lambda_{em} = 460$ nm) was used to label membranes of exosomes and cells. An aliquot of exosomes and cells (about 25 nmol of phospholipids) was incubated for 1 h at room temperature (24 °C) with DPH used at a final concentration of 2 mM in PBS at pH 7.0. When monitoring the effect of pH on exosome fluidity, citrate buffer at pH 4.0, 5.0 or 6.0 was used. The samples were then cooled to 10 °C before fluorescence measurements, which were performed between 15 °C and 40 °C, using a PTI Quantamaster spectrofluorimeter. Anisotropy was then calculated from fluorescence measurements according to the formula described previously [28]. The maximum possible value for DPH anisotropy is 0.362, which would represent an entirely rigid membrane in the gel state.

Derivatization of PE with TNBS (trinitrobenzene sulphonic acid)

The same amount of PE in membranes (i.e. 20 nmol) from exosomes, RBL-2H3 cells, RBCs or LDL (low-density lipoproteins) was used in this experiment. Outer-layer PE from the various samples was derivatized using the non-permeant reagent TNBS (2 mM final concentration) during a 30 min incubation at 4 °C at pH 8.3 according to the method of Hullin et al. [29]. Excess reagent was removed by centrifuging RBL-2H3 cells at 300 ***g*** at 4 °C for 5 min, RBCs at 2000 ***g*** for 10 min at 4 °C and exosomes for 70 min at 110 000 ***g*** at 4 °C. The respective pellets were resuspended in incubation buffer containing 0.5 % (w/v) BSA in order to quench excess TNBS. After further centrifugation under the same conditions as above, the pellets were resuspended in buffer without BSA. Lipids were then extracted and resolved by TLC using the solvent system chloroform/acetone/methanol/ethanoic

acid/ water (5:2:1:1:0.5, by vol.), which allows the separation of derivatized PE from native PE [30]. PE–TNBS and PE were scraped off and their phosphate content was measured as reported above.

ESR

ESR experiments were performed with a Bruker ECJ 106 spectrometer equipped with a resonance cavity TMH 269. The exosomes, LDL and RBCs were labelled with 1 % (v/v) spin label (10^{-2} M) in DMSO to obtain a final ratio of spin label to phospholipids $< 5 \times 10^{-4}$. The spectra were recorded at 24 °C. Each experiment was performed in triplicate and the results shown are the means of the three values. In the hydrophobic part of the different lipidic systems explored with the 16-doxyl stearic acid, we measured the rotational correlation frequency τ_c from the Keith's equation [31], where H_o and W_o are respectively the amplitude and the line width of the central line, H_{+1} the amplitude of the low-field line and H_{-1} that of the high-field line. The amount of paramagnetic probe present in the inner half of the lipidic structures under study (exosomes, LDL, RBCs) was determined as the residual ESR signal after extra-system addition of ice-cold 10 mM sodium ascorbate. In all of our experiments there was at least a 10-fold concentration excess of sodium ascorbate over spin label. The non-reducible label fraction represents the fraction located in the inner leaflet of the lipidic phase [32].

NMR analysis

A chloroformic solution of egg PC (100 mg/ml) was freeze-dried and resuspended in pure ^2H_2O at a final lipid concentration of 10 mM. SUVs (small unilamellar vesicles) were prepared by a 1 h bath sonication. Their integrity was checked by light diffusion and by checking different ^{1}H NMR line widths, as classically described: owing to the small radius of SUVs (10 nm), relatively well resolved lines (10–60 Hz) were detected in the 0.5–5.5 p.p.m. region of ^{1}H NMR spectra (see Figure 5a). This is particularly clear for the resonance attributed to the terminal methyl groups of the acyl chains (0.8 p.p.m., 15 Hz line width) and for the choline $N^+(CH_3)_3$ signal (3.2 p.p.m., 12 Hz line width), the superficial headgroup of lecithin.

^{1}H NMR experiments were carried out on a 400DMX Avance Bruker spectrometer, at 400 MHz and 297 K. A classical presaturation sequence was applied for water suppression. Chemical shifts are referenced to external 3-(trimethylsilyl)propionic-2,2,3,3-d_4 acid sodium salt. A 0.1 M $MnCl_2$ solution (10 μl) was added to preparations to broaden or eliminate all resonances of the external medium.

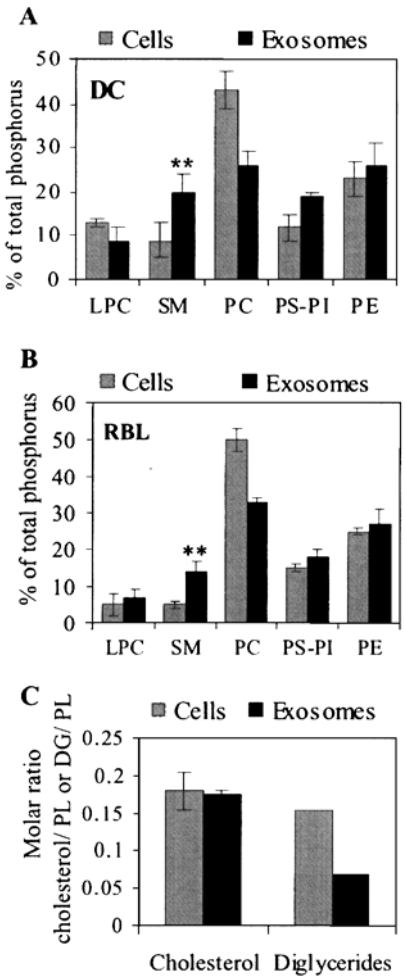

Figure 1 Lipidomic analysis of exosomes isolated from DCs or RBL-2H3 cells

Exosomes were prepared from DCs or RBL-2H3 cells (RBL) as described. Phospholipid classes were separated by TLC using the developing system of Skipski et al. [19]. (**A**) Phospholipid classes from DC-derived exosomes. The data represent the mean for three different experiments ± S.E.M. $^{**}P < 0.02$. (**B**) Phospholipid composition of RBL-2H3-derived exosomes. Data represent the mean for three different experiments ± S.E.M. $^{**}P < 0.02$. (**C**) Neutral lipids from exosomes or RBL-2H3 cells. Results are expressed as the molar ratio between cholesterol or DAGs and total phospholipid (PL) content of lipid extracts. The data represent the mean of three independent experiments ± S.E.M. for cholesterol, and the mean of two independent experiments for DAGs.

RESULTS

Exosomes are vesicles with a specific lipid composition

We first analysed the phospholipid classes and neutral lipids of exosomes as compared with total cells. Data from Figure 1(A) established that exosomes from DCs displayed a balanced phospholipid composition: 26:26:19:20 of PC/PE/PS-PI/SM (in molar percent of total phospholipid) as compared with 43:23:12:9 for DCs. Similarly, in RBL-2H3 cells, the phospholipid distribution between classes was more balanced in exosomes than in the cells from which they were obtained: 33:27:18:14 of PC/PE/PS-PI/SM (molar percent of total phospholipid) in exosomes compared with 50:25:15:5 in RBL-2H3 cells (Figure 1B).

The most striking difference between exosomes and cells concerned the balance between SM and PC. Whatever the origin of the cells, the proportion of SM was twice as high in exosomes as in the corresponding cells, whereas PC was much lower in exosomes than in cells. A small increase was observed for the bulk of PS and PI classes. An increase in both PS and PI taken separately was noticed when using an appropriate solvent (results not shown). Our data also indicated a high LPC content in exosomes, both from RBL-2H3 and DCs.

Regarding neutral lipids (Figure 1C), the DAG-to-phospholipid molar ratio was decreased by 50 % in exosomes. Interestingly, the cholesterol/phospholipid molar ratio was identical between exosomes and RBL-2H3 cells (approx. 0.18). Finally, the lipid composition pattern of exosomes was 1:1:4 for SM/cholesterol/glycerophospholipids (molar ratios), which distinguished them from plasma-membrane rafts whose typical composition has been established as 1:2.2:1.3 [40].

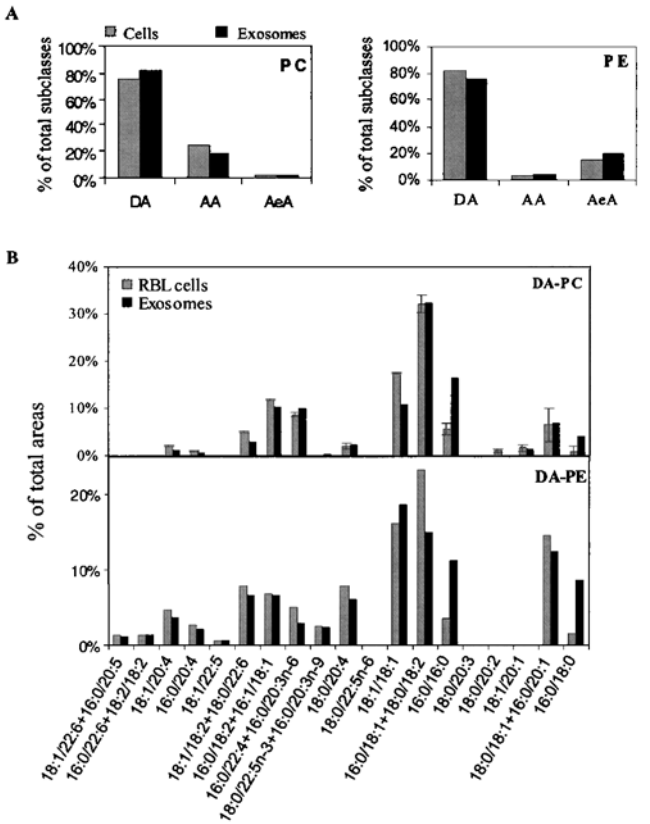

Figure 2 Analysis of molecular species in PC and PE subclasses from RBL-2H3-derived exosomes by HPLC

(**A**) Analysis of PC and PE sub-classes. The two major classes, PC and PE, were separated from total lipid extracts of RBL-2H3 and exosomes as described in the Materials and methods section, and the three subclasses (DA, AA and AeA) were then isolated and quantified by HPLC. Results presented are the mean for two independent experiments. (**B**) Detailed measurement of molecular species in DA-PC or DA-PE subclass. Molecular species from the DA subclass of PC and PE were separated by reverse-phase HPLC as described in the Materials and methods section. Results are the means of two or three independent experiments ± S.E.M.

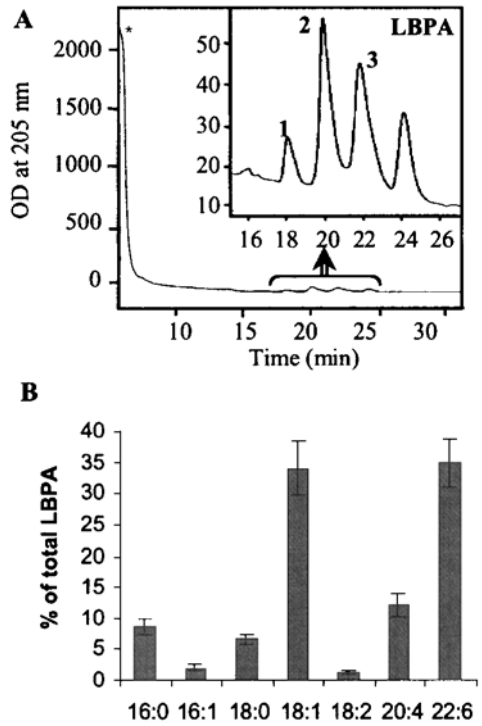

Figure 3 Measurement of LBPA in RBL-2H3 cells

(**A**) Total lipid extracts from RBL-2H3 cells were first resolved by TLC to separate LBPA from most other phospholipids. Then the bulk of LBPA isomers was separated by HPLC from some residual contaminating phospholipids (*), and isomers resolved at retention times between 17 and 25 min. The Figure represents a typical HPLC chromatogram for cells. Similar profiles were obtained from exosomes. The sum of the three peaks (1–3) corresponding to LBPA isomers accounted for the total amount of LBPA (inset). An OD (A_{205}) value of 50 (insert) corresponded to 25 ng of LBPA. (**B**) Fatty-acid composition of cell LBPA. Analysis was by GLC as described in the Materials and methods section. Results are the means for three experiments ± S.E.M.

Because of the limited amount of exosomes recovered from DCs, a more detailed analysis of lipid composition was performed only on RBL-2H3-derived exosomes.

We separated the three major subclasses of PC and PE, i.e. DA, AA and AeA. As shown in Figure 2(A), we did not observe any major difference of proportion between the subclasses of cells and exosomes. More precisely, PC was composed of about 20 % of AA forms, whereas only small amounts of AeA were detected. Typically, an inverse pattern was obtained in PE. In the two classes, DA was the major subclass representing approx. 80 % of the class.

We therefore focused on molecular species analysis of DA-PC and DA-PE subclasses. As shown in Figure 2(B), the most striking differences concerned the proportions of disaturated molecular species, dipalmitoyl ($C_{16:0}/C_{16:0}$) and palmitoyl/stearoyl ($C_{16:0}/C_{18:0}$), which were increased 3–4 times in exosomes as compared with cells. Indeed, the sum of $C_{16:0}/C_{16:0} + C_{16:0}/C_{18:0}$ in DA-PC rose from 6.5 % to 20.6 % between cells and exosomes, and from 5.1 % to 19.8 % in the case of DA-PE (Figure 2B). This increase was subsequent to a net decrease of di-unsaturated species, in PC ($C_{18:1}/C_{18:1}$) or mono-unsaturated species ($C_{16:0}/C_{18:1} + C_{18:0}/C_{18:2}$) in PE of exosomes as compared with cells.

Then LBPA, a phospholipid essentially localized in MVBs, was considered. Using UV detection following HPLC separation, we detected the three isomers of LBPA in cells (Figure 3A) as well as in exosomes (results not shown). The fatty-acid composition of LBPA was then analysed by GLC. As shown in Figure 3(B), in RBL-2H3 cells, the most enriched fatty acids are DHA ($C_{22:6}$) and oleic acid ($C_{18:1}$) as previously shown in rat uterine stromal cells [20]. However, there was no enrichment of LBPA in exosomes as compared with RBL-2H3 cells, since LBPA accounted for 0.8 % and 1.2 % of total phospholipids for exosomes and cells respectively. ELISAs using the 6C4 antibody directed against LBPA [11] confirmed these results (results not shown).

Therefore exosomes from mast cells appear to correspond to a new type of lipid membrane with high levels of SM and di-saturated glycerophospholipid molecular species, but without any enrichment in cholesterol or LBPA as compared with total cells.

Analysis of exosome-membrane fluidity

Enrichment of SM and disaturated phospholipids in exosomes suggested tight lipid packing in these membranes. To confirm this, membrane fluidity of RBL-2H3-derived exosomes was analysed by monitoring fluorescence anisotropy of a hydrophobic probe, DPH, i.e. the capacity of this probe to move in its lipid surroundings (Figure 4). The higher the anisotropy value, the higher the rigidity of the membranes [28]. DPH labelled mostly plasma membranes when added to intact cells (results not shown). Because the pH of the medium surrounding exosomes is shifted from 5 (in MVBs) to 7 when they are released in the

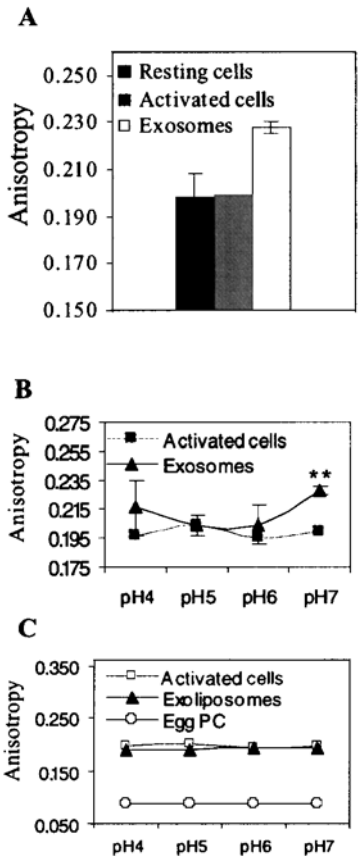

Figure 4 Analysis of exosome- and cell-membrane fluidity by fluorescence polarization measurement

(**A**) Membrane fluidity was analysed by fluorescence anisotropy of the hydrophobic fluorescent probe DPH in membranes. DPH was incubated with intact exosomes, or resting or activated cells. Fluorescence anisotropy was measured at various temperatures by polarization fluorescence (see the Materials and methods section). The Figure shows the comparative anisotropy between exosomes and cells at the physiological temperature of 37 °C. Maximum possible anisotropy for DPH is 0.362. The results are the means for three independent experiments ± S.E.M. (**B**, **C**) Fluorescence anisotropy as a function of pH. Cells and exosomes (**B**), or exoliposomes and PC-liposomes (**C**), were suspended in buffer at the appropriate pH values. Anisotropy was measured at 37 °C as in (**A**). $^{**}P < 0.05$.

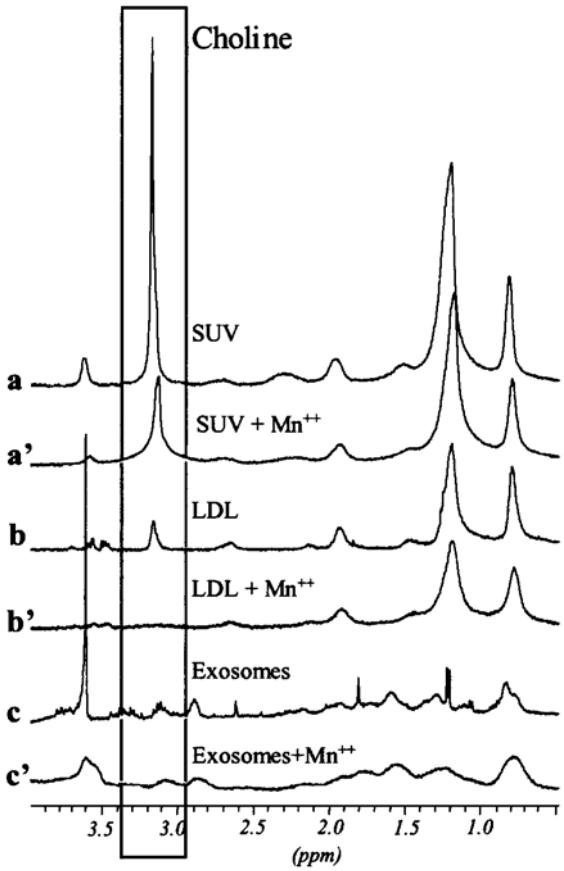

Figure 5 NMR spectra of exosomes compared with monolayer (LDL) or bilayer (SUVs) membrane

^{1}H NMR experiments were carried out on exosomes and SUVs or LDL in the absence or presence of Mn^{2+} as a quenching agent. We observed that, in the presence of Mn^{2+}, all the peaks from the exosome spectrum were widened, due to the accessibility of the reagent. This was the case for the choline peak at 3.2 p.p.m. The other peaks could not be attributed specifically to a particular class of molecule (i.e. lipid or protein). Mn^{2+} quenched the choline signal only in the LDL sample. The Figure represents the 0.5–4 p.p.m. regions of spectra.

outer-cell medium, we analysed their membrane fluidity according to pH.

At neutral pH (Figure 4A), exosome membranes exhibited a significantly higher anisotropy (0.230) than plasma membranes of resting or activated cells (0.195). This value of 0.230 for exosome anisotropy at 37 °C corresponded to that of cells incubated at 24 °C (results not shown). The increase from 0.195 to 0.230 is dynamically significant, since the maximum anisotropy value for DPH is 0.362, corresponding to a gel-state membrane. However, when checked at lower pH, exosome rigidity was quite similar to that of cell plasma membrane (Figure 4B). Comparatively, the rigidity of plasma membrane of activated cells remained constant across pH. It was concluded that some membrane reorganization occurred in exosomes between the acidic environment of MVB and the neutral pH of the outer-cell medium.

In order to estimate the respective roles of proteins and lipids in exosome-membrane fluidity, DPH fluorescence anisotropy was measured on liposomes having the same composition as the lipid phase of natural exosomes (exoliposomes). The anisotropy of exoliposomes was similar to that of RBL-2H3 cells, and much higher than that of liposomes containing only PC (Figure 4C). In any case, no change in fluidity was noted as a function of pH. Thus protein organization in natural exosomes accounts for a large part of the increase in membrane rigidity from pH 5 to 7.

Analysis of exosome-membrane organization

In order to investigate exosome-membrane organization further, we performed proton NMR and ESR analysis in the presence or absence of agents that specifically quenched signals from the outer leaflet. RBCs and LDL were used for bilayer and monolayer controls respectively. Figure 5 represents exosome ^{1}H NMR spectra with and without paramagnetic Mn^{2+} ions (Figures 5c and 5c' respectively), compared with SUVs (Figures 5a and 5a') and LDL (Figures 5b and 5b') spectra. For SUVs, the $N^+(CH_3)_3$ group resonance of the outer leaflet component was broadened beyond detection after addition of Mn^{2+}, while the inner leaflet component was not significantly affected. In this way, the bilayer arrangement of phospholipids in SUVs was unambiguously confirmed. Conversely, choline resonance completely vanished from the LDL spectrum when Mn^{2+} was added, indicating that all headgroups were accessible to this ion (Figure 5b'), and consistent with the monolayer organization of phospholipids in this lipoprotein.

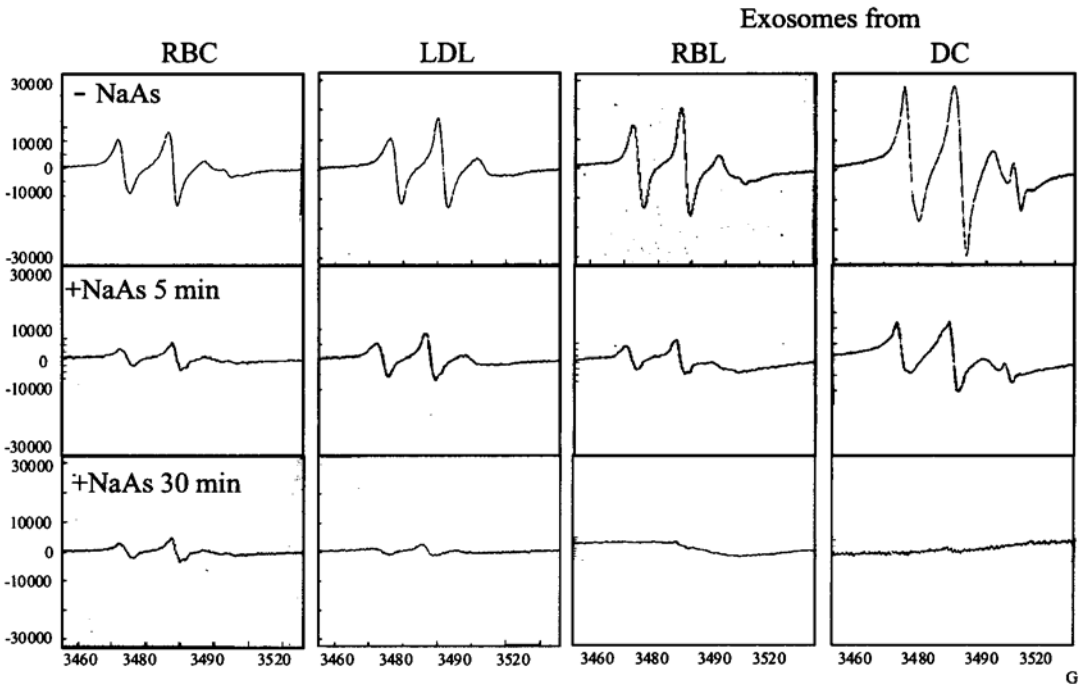

Figure 6 ESR spectra of exosomes from RBL-2H3 cells or from DCs

RBCs and LDL were used as controls for bilayer and monolayer membranes. The experimental conditions were the same in the three types of experiments, as described in the Materials and methods section. After incubation with the paramagnetic probe, 16-doxyl stearic acid, resonance was measured from the four samples in the presence or absence of sodium ascorbate (NaAs), a quenching agent, after 5 and 30 min of incubation. Results are expressed as arbitrary units after spectrum normalization. Magnetic field values are plotted on the abscissa.

The global broadening of the exosome resonances when paramagnetic ions are present in the external medium (Figure 5c') indicates that all the protons are accessible to this ion, i.e. that none of them are completely buried. It must be recalled that the attribution of the complete spectrum to either proteins or lipids was difficult, since their respective resonances are not separate. However, the choline peak was not entirely abolished in the presence of Mn^{2+}, demonstrating that the lipid phase of the exosomes was organized as a bilayer.

We next analysed the signal recovered from 16-doxyl stearic fatty acid inserted into membranes, by ESR. Results shown in Figure 6 (upper panels) were typical of a 16-doxyl stearic acid signal. In the presence of sodium ascorbate, a non-permeant reducer which quenches only the signal accessible on the outer layer [32], the profiles were attenuated after 5 min of treatment at 10 °C (Figure 6, middle panels). After 30 min of treatment with sodium ascorbate, the residual spectrum in RBCs was similar to that obtained after 5 min of treatment and was consistent with a bilayer membrane, whereas almost no signal was recovered from the monolayer membrane of the LDL sample (Figure 6, lower panels). The remaining shoulder in LDL after 30 min of treatment indicated some amount of 16-doxyl stearic acid incorporated into the neutral lipid core of the lipoprotein. We then analysed the signals recovered both from exosomes derived from RBL-2H3 cells and exosomes recovered from DCs after 30 min of treatment with ascorbate. We observed complete extinction of the signals in the presence of sodium ascorbate both in RBL-2H3- and DC-derived exosomes (Figure 6, lower panels), indicating the complete accessibility of the doxyl probe to the reducing reagent in exosomes. This observation indicated a higher transmembrane flip-flop of lipids in exosomes than in a regular bilayer, such as the RBC membrane.

Together, NMR and ESR studies demonstrated a bilayer organization of exosome membrane with high transmembrane lipid diffusion.

Transmembrane distribution of PE in exosomes

Results from ESR studies prompted us to investigate exosome transmembrane organization more thoroughly. The transverse phospholipid distribution was approached by measuring the amount of PE accessible to the non-permeant reagent TNBS. This method has been widely used to determine amino-containing phospholipid asymmetry in membranes [29]. Our results in Figure 7 demonstrate that in RBCs, taken as a control of a bilayer membrane, most of the PE class is located in the inner leaflet, in agreement with the literature [33]. Also, in intact RBL-2H3 cells, most of the PE was in the inner plasma membrane leaflet together with the intracellular membranes. Instead, $> 50\,\%$ of the PE was derivatized by TNBS in exosomes, compared with 75 % for PE in LDL, taken as a control of a monolayer membrane. We checked that 100 % of PE was accessible to TNBS in either sample when the derivatization was performed in methanol, which destroyed membrane asymmetry; this indicated that the amount of reagent was not a limiting step in the derivatization reaction. Therefore the results obtained for LDL indicated the limitation of TNBS accessibility towards PE present in a biological membrane. The results in Figure 7(A) were thus corrected by taking the amount of PE in the LDL monolayer as 100 % and plotted in Figure 6(B). In a liposome of 60 nm diameter, i.e. with a size similar to that of exosomes, roughly two thirds of the phospholipids are located on the outer leaflet. Therefore the results in Figure 7(B) reporting 70 % PE on exosome outer leaflet were compatible with a vesicle in which the asymmetrical distribution of phospholipids was lost.

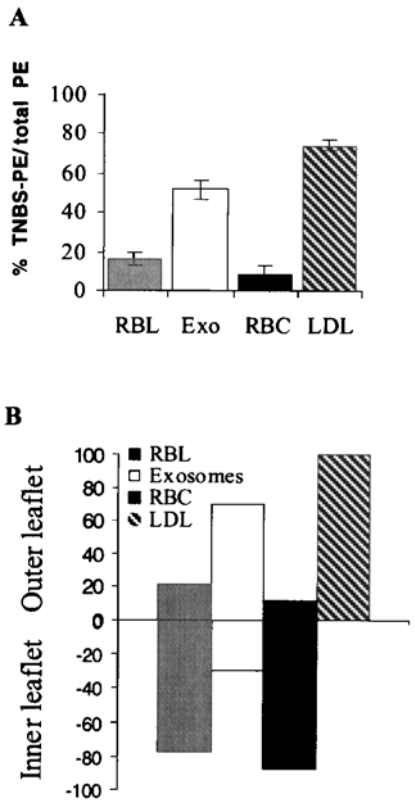

Figure 7 Transmembrane distribution of PE in exosomes

RBL-2H3 cells, RBL-2H3-derived exosomes, RBCs (bilayer membrane) and LDLs (monolayer membrane) were incubated with TNBS at 4 °C for 30 min. Excess compound was removed and, after lipid extraction, conjugated TNBS–PE were separated from residual PE and other phospholipids by TLC using an appropriate solvent (see the Materials and methods section). Results are expressed as a percentage of TNBS-PE over total PE (**A**). In (**B**), the transmembrane distribution of PE in each sample was normalized by taking the amount of PE-TNBS in LDL as 100 %.

DISCUSSION

Exosomes have been shown to stimulate the immune system and, more precisely, to stimulate T-lymphocytes both *in vivo* and *in vitro* [2,34]. *In vitro*, this stimulation is dependent on DCs [12]. More recently, it has been shown that exosomes from mast cells have the ability to induce phenotypic and functional maturation of DCs [13]. Mechanisms underlying these immunological properties are not clearly understood at the moment, but characterization of proteins and lipids present on exosomes could help to elucidate them. To complement proteomic analyses [5,35] and morphological descriptions [8,15] of exosomes from various cell types, lipid and structural analyses on exosomes from RBL-2H3, a mast cell line, and from human DCs were carried out.

In the present study, it was established that exosomes from these two cell types have a specific phospholipid composition different from that of the parent cells; major phospholipids and cholesterol level off at approx. 20–30 % (in molar percent of total). Moreover, the class of SM is increased approx. 2-fold in exosome membranes as compared with cell membranes (Figure 1B). This is in agreement with a similar increase reported in B-cell-line-derived exosomes [36]. Therefore a high SM content appears to be a general feature of exosomes.

In order to characterize in more detail the lipid phase of exosomes, molecular species of the major phospholipids, PC and PE were analysed. The general pattern of molecular species in Figure 2(B) is consistent with those obtained from other haematopoietic cells [24,37], or even cells of distinct cell lineage such as fibroblasts [38], using the same procedure of subclass separation and derivatization. Instead, a study on RBL-2H3 cells using electrospray ionization MS on total PC and PE classes [39] reports some differences with our results, since they have observed more polyunsaturated species and could barely detect di-saturated ones. These discrepancies might depend upon culture conditions. Regarding di-saturated species in Figure 2, the amount of $C_{16:0}/C_{16:0} + C_{16:0}/C_{18:0}$ represents 6 % in PC and 5 % in PE; values in agreement with those reported in DA-PC of thymocytes [24] or DA-PE of platelets [37]. Thus the net increase in saturated species both in PC and PE of exosomes is a feature of these vesicles. It should be borne in mind that these same species account for up to 40 % of the total PC class in platelets, as measured either by HPLC following derivatization or by desorption-chemical soft ionization-MS [37].

Regarding neutral lipids, we have observed in RBL-2H3-derived exosomes that DAGs are present in about half the amount found in cells. These three parameters, i.e. a high content of SM, di-saturated molecular species and decreased DAGs, are known to affect lipid packing in membranes.

Since the amount of cholesterol in exosomes secreted by RBL-2H3 cells was identical with that of cells, it can be concluded that RBL-2H3-derived exosomes are distinct from cholesterol-enriched lipid microdomains, termed 'rafts'. In the case of rafts, lipid composition exhibits a high cholesterol/phospholipids molar ratio (1.2), together with a high SM content, whereas glycerophospholipids are minor constituents [40]. Recently, an enrichment in cholesterol has been reported in exosomes derived from a lymphoid B-cell line [36]; results that differ from those obtained in the present study. In the present study, we used other cell models which belong to myeloid lineage, a rat mast cell line (RBL-2H3) known to secrete immunocompetent exosomes [4,12], and DC-derived exosomes of human origin. Nevertheless, it is possible that tiny microdomains exist on exosome membranes from RBL-2H3 mast cells resulting from a local increase in cholesterol. In the present study, exosomes feature an increase in SM content leading to a final 1:1 stoichiometric ratio between cholesterol and SM. Studies on fusogenic liposomes have suggested such a ratio could be important for membrane stabilization in minimizing rupture, while maximizing fusion [41]. This is in agreement with the observed resistance of exosomes to freezing–thawing cycles (results not shown) and would support the ability of exosomes to fuse with other membranes, although such a fusion process has not been observed so far.

Regarding LBPA, known to be localized on luminal membranes of MVBs [42], no enrichment was observed on secreted exosomes after HPLC quantification. Using the 6C4 antibody [11], we were also unable to detect any enrichment of this lipid. These results could be explained if a recent study indicating that different subpopulations of late endosomes (also called MVBs) are present within the cells, and that only some of them contain a noticeable amount of LBPA [43], is taken into account. We suggest that exosomes are released only from MVB with low LBPA content. In this respect, B-cell-derived exosomes were not enriched in LBPA either [36].

It has also been observed in the present study that the proportion of LPC is relatively high in exosomes and in cells, more precisely in DCs (Figure 1). The presence of LPC in exosomes might be essential for their activity *in vivo*, since LPC [44] and exosomes [13] trigger DC maturation. This biological effect might proceed via a recently characterized LPC receptor named G2A [45], and be involved in the immune response, since $G2A^{-/-}$ mice develop an autoimmune disease [46].

Interestingly, lipid analyses of exosomes have shown that they display a similar phospholipid composition even though they are secreted by two different cell types, i.e. RBL-2H3 cells, a tumoral mast cell line from rats, and bone-marrow-derived DCs of human origin. In addition, this lipid composition seems to be independent of the secretion pathway, since exosomes from DCs are constitutively secreted, whereas exosomes from RBL-2H3 cells are released following stimulation of a 'regulated pathway'.

The phospholipid composition that has been established in the present study has led to the suspicion of specific dynamics for exosome membranes. Indeed, SM has been shown to decrease fluidity [47] due to the nature of their acyl chains, which are mostly saturated and longer than in glycerophospholipids [47]. In the same way, the increase of disaturated molecular species among the PC and PE also accounts for exosome rigidity. Our values on RBL-2H3 cell anisotropy (0.195; Figure 4A) are consistent with previous studies performed on the same cells [48]. It can be concluded from Figure 4(A) that exosomes display a significantly higher rigidity than RBL-2H3 cell plasma membranes. The significant increase in exosome-membrane rigidity that is observed between pH 5 and pH 7 suggests a modification of exosome-membrane organization at the time they switch from an acidic to a neutral environment (Figure 4B), which occurs when they are released from acidic MVBs to the outer-cell medium. This high membrane rigidity at neutral pH can explain the stability of the immune properties of exosomes from DCs observed during storage and clinical trials. In the same way, the initial study of Zitvogel et al. [2] in mice describing exosomes as a tool against tumour growth suggests that these vesicles are very stable in a whole organism, since one shot of 100 μg of exosomes is able to eradicate a mastocytoma grown for 2 months. Proteins in exosomes can partly account for this membrane increase in rigidity, since the anisotropy of the lipid phase alone (exoliposomes) remains constant with pH (Figure 4C). Exosomes are highly enriched in tetraspanins, which might be organized in microdomains distinct from lipid rafts [49] in a possible pH-dependent process. It is noteworthy that, in RBL-2H3-derived plasma-membrane vesicles, the protein content has no influence on DPH anisotropy values [48].

Although biological plasma membranes are organized in a bilayer, nothing is known about the membrane organization of a vesicle originating from MVBs, such as exosomes. LBPA, a cone-shaped lipid, might trigger some particular lipid organization during exosome biogenesis inside MVBs, even though we have shown that the LBPA present in MVBs is not transferred on to exosomes. NMR results have confirmed a classical bilayer membrane organization in exosomes. Surprisingly, however, the entire signal from doxyl stearic acid in ESR experiments was quenched in exosomes after 30 min of ascorbic acid treatment. Therefore our results in Figures 5 and 6 characterized exosome membrane by a rapid transmembrane flip-flop of lipids between the two leaflets. This hypothesis was confirmed by results on PE transmembrane distribution. The results shown in Figure 7 have shown that PE in exosome membrane is randomly distributed between the two leaflets, whereas its asymmetric distribution in the inner leaflet of plasma membrane is well established [50].

This non-asymmetrical distribution of PE on exosomes allows them to be discriminated from other biological vesicles that originate from plasma-membrane shedding, for example [50].

Taken together, these results lead to an apparent paradox between the great rigidity of exosome membranes and the high rate of phospholipid flip-flop between the two membrane leaflets. According to Homan and Pownall [51], the apolar portion of phospholipids has less importance than the polar headgroup in transbilayer movements [51]. This indicates that high levels of saturated-fatty-acid-containing phospholipids in a membrane leaflet would not prevent transbilayer movement of the lipids. In addition, flip-flop rate is largely dependent upon the intracellular or plasma-membrane origin of the membrane. Flip-flop in plasma membrane is very slow (a $t_{1/2}$ in hours or days) [51] and is limited by a flippase, which actively maintains phospholipid asymmetry [52]. In contrast, the transbilayer motion of phospholipids in endoplasmic reticulum (ER) membranes is faster (a $t_{1/2}$ in seconds or minutes) [51,52], and is dependent upon a protein-mediated transport process leading to a symmetric transbilayer distribution of phospholipids [53,54]. The same mechanism seems to occur in Golgi apparatus [54], which participates in some way to MVB biogenesis [55]. Indeed, we have observed that a fluorescent lipid marker of Golgi complex in RBL-2H3 cells [BODIPY® (4,4-difluoro-4-bora-3*a*,4*a*-diaza-*s*-indacene)–ceramide] could also be recovered in exosomes (K. Laulagnier and M. Record, unpublished work). Since exosomes are generated from MVBs, it is conceivable that the flip-flop rate in their membranes would be closer to that of ER or Golgi bodies than that of plasma membrane. This hypothesis is in agreement with the symmetric PE distribution that we have observed in exosomes. Moreover, proteomic analysis of DC-derived exosomes has not detected any plasma-membrane flippase [5], which is consistent with the lack of membrane asymmetry. On the other hand, the above-mentioned protein carrying lipid-translocation activity observed in ER is still not characterized at the molecular level and therefore is not available in proteomic databases.

The dynamics and organization of exosome membrane certainly accounts for their original immune activity. The membrane rigidity at pH 7 certainly prevents lipolytic or proteolytic degradation of exosomes in the circulation. We have shown that exosomes display a specific lipid composition, with lateral diffusion lower than in a plasma membrane, but with higher transbilayer movements, consistent with loss of phospholipid asymmetry. In that respect, it has been demonstrated that asymmetry of phospholipids in plasma membranes is critical in the membrane fusion underlying the degranulation of RBL-2H3 cells [56]. Then, the loss of phospholipid asymmetry that we observed in exosomes could explain why they are not able to fuse with target plasma membranes of follicular DCs, but are only adsorbed on them [57]. This adsorption allows follicular DCs to recover appropriate antigen presentation [57]. Finally, exosome lipid dynamics and protein domains, such as tetraspanin domains, could be essential to keep immune proteins, such as MHC class II in an optimal and functional conformation.

We thank Chantal Thevenon (Insa, Lyon, France) and Nadège Briche (U563 Toulouse, France) for molecular species analysis; Danièle Lankar (U520, Paris, France) for electron microscopy of exosomes; Jean-Claude Debouzy (CRSSA, Grenoble, France) for NMR studies, and Alain Zachowski and Claude Wolf (Paris, France) for their critical comments on NMR and ESR experiments. This work was initiated under the European BIOMED 2 program, which also supported S.R., and was further funded by the Ligue Nationale Contre le Cancer (Comité du Tarn et Garonne, France), and partly by the GenHomme project (MENRT, France). K.L. was supported by a grant from MENRT and Association pour la Recherche contre le Cancer, and S.H. in part by Fondation de la Recherche Medicale (France).

REFERENCES

1 Denzer, K., Kleijmeer, M. J., Heijnen, H. F., Stoorvogel, W. and Geuze, H. J. (2000) Exosome: from internal vesicle of the multivesicular body to intercellular signaling device. J. Cell. Sci. **113**, 3365–3374

2 Zitvogel, L., Regnault, A., Lozier, A., Wolfers, J., Flament, C., Tenza, D., Ricciardi-Castagnoli, P., Raposo, G. and Amigorena, S. (1998) Eradication of established murine tumors using a novel cell-free vaccine: dendritic cell-derived exosomes. Nat. Med. **4**, 594–600

3 Andre, F., Andersen, M., Wolfers, J., Lozier, A., Raposo, G., Serra, V., Ruegg, C., Flament, C., Angevin, E., Amigorena, S. and Zitvogel, L. (2001) Exosomes in cancer immunotherapy: preclinical data. Adv. Exp. Med. Biol. **495**, 349–354

4 Raposo, G., Tenza, D., Mecheri, S., Peronet, R., Bonnerot, C. and Desaymard, C. (1997) Accumulation of major histocompatibility complex class II molecules in mast cell secretory granules and their release upon degranulation. Mol. Biol. Cell **8**, 2631–2645

5 Thery, C., Boussac, M., Veron, P., Ricciardi-Castagnoli, P., Raposo, G., Garin, J. and Amigorena, S. (2001) Proteomic analysis of dendritic cell-derived exosomes: a secreted subcellular compartment distinct from apoptotic vesicles. J. Immunol. **166**, 7309–7318

6 Escola, J. M., Kleijmeer, M. J., Stoorvogel, W., Griffith, J. M., Yoshie, O. and Geuze, H. J. (1998) Selective enrichment of tetraspan proteins on the internal vesicles of multivesicular endosomes and on exosomes secreted by human B-lymphocytes. J. Biol. Chem. **273**, 20121–20127

7 Boucheix, C. and Rubinstein, E. (2001) Tetraspanins. Cell. Mol. Life Sci. **58**, 1189–1205

8 Stoorvogel, W., Kleijmeer, M. J., Geuze, H. J. and Raposo, G. (2002) The biogenesis and functions of exosomes. Traffic **3**, 321–330

9 Fernandez-Borja, M., Wubbolts, R., Calafat, J., Janssen, H., Divecha, N., Dusseljee, S. and Neefjes, J. (1999) Multivesicular body morphogenesis requires phosphatidyl-inositol 3-kinase activity. Curr. Biol. **9**, 55–58

10 Futter, C. E., Collinson, L. M., Backer, J. M. and Hopkins, C. R. (2001) Human VPS34 is required for internal vesicle formation within multivesicular endosomes. J. Cell Biol. **155**, 1251–1264

11 Kobayashi, T., Stang, E., Fang, K. S., de Moerloose, P., Parton, R. G. and Gruenberg, J. (1998) A lipid associated with the antiphospholipid syndrome regulates endosome structure and function. Nature (London) **392**, 193–197

12 Vincent-Schneider, H., Stumptner-Cuvelette, P., Lankar, D., Pain, S., Raposo, G., Benaroch, P. and Bonnerot, C. (2002) Exosomes bearing HLA-DR1 molecules need dendritic cells to efficiently stimulate specific T cells. Int. Immunol. **14**, 713–722

13 Skokos, D., Botros, H. G., Demeure, C., Morin, J., Peronet, R., Birkenmeier, G., Boudaly, S. and Mecheri, S. (2003) Mast cell-derived exosomes induce phenotypic and functional maturation of dendritic cells and elicit specific immune responses *in vivo*. J. Immunol. **170**, 3037–3045

14 Lamparski, H. G., Metha-Damani, A., Yao, J. Y., Patel, S., Hsu, D. H., Ruegg, C. and Le Pecq, J. B. (2002) Production and characterization of clinical grade exosomes derived from dendritic cells. J. Immunol. Methods **270**, 211–226

15 Raposo, G., Nijman, H. W., Stoorvogel, W., Liejendekker, R., Harding, C. V., Melief, C. J. and Geuze, H. J. (1996) B lymphocytes secrete antigen-presenting vesicles. J. Exp. Med. **183**, 1161–1172

16 Lowry, O. H., Rosebrough, N. J., Farr, A. L. and Randall, R. J. (1951) Protein measurement with the folin phenol reagent. J. Biol. Chem. **193**, 265–275

17 Bligh, E. G. and Dyer, W. J. (1959) A rapid method for total lipid extraction and purification of phospholipids. Can. J. Biochem. Physiol. **37**, 911–918

18 Böttcher, C. J. F., Van Gent, C. M. and Pries, C. (1961) A rapid and sensitive sub-micro phosphorus determination. Anal. Clin. Acta **24**, 203–204

19 Skipski, V. P., Peterson, R. F. and Barclay, M. (1964) Quantitative analysis of phospholipids by thin-layer chromatography. Biochem. J. **90**, 374–378

20 Luquain, C., Dolmazon, R., Enderlin, J. M., Laugier, C., Lagarde, M. and Pageaux, J. F. (2000) Bis(monoacylglycerol) phosphate in rat uterine stromal cells: structural characterization and specific esterification of docosahexaenoic acid. Biochem. J. **351**, 795–804

21 Thevenon, C., El Bawab, S., Chantegrel, B. and Lagarde, M. (1998) Highly sensitive measurement of lipid molecular species from biological samples by fluorimetric detection coupled to high-performance liquid chromatography. J. Chromatogr. B. Biomed. Sci. Appl. **708**, 39–47

22 Arduini, A., Peschechera, A., Dottori, S., Sciarroni, A. F., Serafini, F. and Calvani, M. (1996) High performance liquid chromatography of long-chain acylcarnitine and phospholipids in fatty acid turnover studies. J. Lipid Res. **37**, 684–689

23 Ramesha, C. S., Pickett, W. C. and Murthy, D. V. (1989) Sensitive method for the analysis of phospholipid subclasses and molecular species as 1-anthroyl derivatives of their diglycerides. J. Chromatogr. **491**, 37–48

24 El Bawab, S., Macovschi, O., Thevenon, C., Goncalves, A., Nemoz, G., Lagarde, M. and Prigent, A. F. (1996) Contribution of phosphoinositides and phosphatidylcholines to the production of phosphatidic acid upon concanavalin A stimulation of rat thymocytes. J. Lipid Res. **37**, 2098–2108

25 Luquain, C., Laugier, C., Lagarde, M. and Pageaux, J. F. (2001) High-performance liquid chromatography determination of bis(monoacylglycerol) phosphate and other lysophospholipids. Anal. Biochem. **296**, 41–48

26 Felouati, B. E., Pageaux, J. F., Fayard, J. M., Lagarde, M. and Laugier, C. (1994) Oestradiol-induced changes in the composition of phospholipid classes of quail oviduct: specific replacement of arachidonic acid by docosahexaenoic acid in alkenylacyl-glycerophosphoethanolamine. Biochem. J. **301**, 361–366

27 Vieu, C., Jaspard, B., Barbaras, R., Manent, J., Chap, H., Perret, B. and Collet, X. (1996) Identification and quantification of diacylglycerols in HDL and accessibility to lipase. J. Lipid Res. **37**, 1153–1161

28 Shinitzky, M. and Inbar, M. (1976) Microviscosity parameters and protein mobility in biological membranes. Biochim. Biophys. Acta **433**, 133–149

29 Hullin, F., Bossant, M. J. and Salem, Jr, N. (1991) Aminophospholipid molecular species asymmetry in the human erythrocyte plasma membrane. Biochim. Biophys. Acta **1061**, 15–25

30 Vale, M. G. (1977) Localization of the amino phospholipids in sarcoplasmic reticulum membranes revealed by trinitrobenzenesulfonate and fluorodinitrobenzene. Biochim. Biophys. Acta **471**, 39–48

31 Keith, A. D., Sharnoff, M. and Cohn, G. E. (1973) A summary and evaluation of spin labels used as probes for biological membrane structure. Biochim. Biophys. Acta **300**, 379–419

32 Seigneuret, M., Zachowski, A., Hermann, A. and Devaux, P. F. (1984) Asymmetric lipid fluidity in human erythrocyte membrane: new spin-label evidence. Biochemistry **23**, 4271–4275

33 Schroit, A. J. and Zwaal, R. F. (1991) Transbilayer movement of phospholipids in red cell and platelet membranes. Biochim. Biophys. Acta **1071**, 313–329

34 Wolfers, J., Lozier, A., Raposo, G., Regnault, A., Thery, C., Masurier, C., Flament, C., Pouzieux, S., Faure, F., Tursz, T. et al. (2001) Tumor-derived exosomes are a source of shared tumor rejection antigens for CTL cross-priming. Nat. Med. **7**, 297–303

35 Thery, C., Regnault, A., Garin, J., Wolfers, J., Zitvogel, L., Ricciardi-Castagnoli, P., Raposo, G. and Amigorena, S. (1999) Molecular characterization of dendritic cell-derived exosomes: selective accumulation of the heat shock protein hsc73. J. Cell Biol. **147**, 599–610

36 Wubbolts, R., Leckie, R. S., Veenhuizen, P. T., Schwarzmann, G., Mobius, W., Hoernschemeyer, J., Slot, J. W., Geuze, H. J. and Stoorvogel, W. (2003) Proteomic and biochemical analyses of human B cell-derived exosomes: potential implications for their function and multivesicular body formation. J. Biol. Chem. **278**, 10963–10972

37 Masrar, H., Bereziat, G. and Colard, O. (1990) Very high proportion of disaturated molecular species in rat platelet diacyl-glycerophosphocholine: involvement of CoA-dependent transacylation reactions. Arch. Biochem. Biophys. **281**, 116–123

38 Pettitt, T. R. and Wakelam, M. J. (1993) Bombesin stimulates distinct time-dependent changes in the *sn*-1,2-diradylglycerol molecular species profile from Swiss 3T3 fibroblasts as analysed by 3,5-dinitrobenzoyl derivatization and h.p.l.c. separation. Biochem. J. **289**, 487–495

39 Ivanova, P. T., Cerda, B. A., Horn, D. M., Cohen, J. S., McLafferty, F. W. and Brown, H. A. (2001) Electrospray ionization mass spectrometry analysis of changes in phospholipids in RBL-2H3 mastocytoma cells during degranulation. Proc. Natl. Acad. Sci. U.S.A. **98**, 7152–7157

40 Bodin, S., Giuriato, S., Ragab, J., Humbel, B. M., Viala, C., Vieu, C., Chap, H. and Payrastre, B. (2001) Production of phosphatidylinositol 3,4,5-trisphosphate and phosphatidic acid in platelet rafts: evidence for a critical role of cholesterol-enriched domains in human platelet activation. Biochemistry **40**, 15290–15299

41 Haque, M. E., McIntosh, T. J. and Lentz, B. R. (2001) Influence of lipid composition on physical properties and PEG-mediated fusion of curved and uncurved model membrane vesicles: "Nature's own" fusogenic lipid bilayer. Biochemistry **40**, 4340–4348

42 Kobayashi, T., Gu, F. and Gruenberg, J. (1998) Lipids, lipid domains and lipid-protein interactions in endocytic membrane traffic. Semin. Cell Dev. Biol. **9**, 517–526

43 Kobayashi, T., Beuchat, M. H., Chevallier, J., Makino, A., Mayran, N., Escola, J. M., Lebrand, C., Cosson, P. and Gruenberg, J. (2002) Separation and characterization of late endosomal membrane domains. J. Biol. Chem. **277**, 32157–32164

44 Coutant, F., Perrin-Cocon, L., Agaugue, S., Delair, T., Andre, P. and Lotteau, V. (2002) Mature dendritic cell generation promoted by lysophosphatidylcholine. J. Immunol. **169**, 1688–1695

45 Kabarowski, J. H., Zhu, K., Le, L. Q., Witte, O. N. and Xu, Y. (2001) Lysophosphatidylcholine as a ligand for the immunoregulatory receptor G2A. Science **293**, 702–705

46 Le, L. Q., Kabarowski, J. H., Weng, Z., Satterthwaite, A. B., Harvill, E. T., Jensen, E. R., Miller, J. F. and Witte, O. N. (2001) Mice lacking the orphan G protein-coupled receptor G2A develop a late-onset autoimmune syndrome. Immunity **14**, 561–571

47 Holthuis, J. C., Pomorski, T., Raggers, R. J., Sprong, H. and Van Meer, G. (2001) The organizing potential of sphingolipids in intracellular membrane transport. Physiol. Rev. **81**, 1689–1723

48 Gidwani, A., Holowka, D. and Baird, B. (2001) Fluorescence anisotropy measurements of lipid order in plasma membranes and lipid rafts from RBL-2H3 mast cells. Biochemistry **40**, 12422–12429

49 Kropshofer, H., Spindeldreher, S., Rohn, T. A., Platania, N., Grygar, C., Daniel, N., Wolpl, A., Langen, H., Horejsi, V. and Vogt, A. B. (2002) Tetraspan microdomains distinct from lipid rafts enrich select peptide-MHC class II complexes. Nat. Immunol. **3**, 61–68
50 Zachowski, A. (1993) Phospholipids in animal eukaryotic membranes: transverse asymmetry and movement. Biochem. J. **294**, 1–14
51 Homan, R. and Pownall, H. J. (1988) Transbilayer diffusion of phospholipids: dependence on headgroup structure and acyl chain length. Biochim. Biophys. Acta **938**, 155–166
52 Herrmann, A., Zachowski, A. and Devaux, P. F. (1990) Protein-mediated phospholipid translocation in the endoplasmic reticulum with a low lipid specificity. Biochemistry **29**, 2023–2027
53 Buton, X., Morrot, G., Fellmann, P. and Seigneuret, M. (1996) Ultrafast glycerophospholipid-selective transbilayer motion mediated by a protein in the endoplasmic reticulum membrane. J. Biol. Chem. **271**, 6651–6657

Received 20 October 2003/12 February 2004; accepted 13 February 2004
Published as BJ Immediate Publication 13 February 2004, DOI 10.1042/BJ20031594

54 Buton, X., Herve, P., Kubelt, J., Tannert, A., Burger, K. N., Fellmann, P., Muller, P., Herrmann, A., Seigneuret, M. and Devaux, P. F. (2002) Transbilayer movement of monohexosylsphingolipids in endoplasmic reticulum and Golgi membranes. Biochemistry **41**, 13106–13115
55 Sorkin, A. and Von Zastrow, M. (2002) Signal transduction and endocytosis: close encounters of many kinds. Nat. Rev. Mol. Cell Biol. **3**, 600–614
56 Kato, N., Nakanishi, M. and Hirashima, N. (2002) Transbilayer asymmetry of phospholipids in the plasma membrane regulates exocytotic release in mast cells. Biochemistry **41**, 8068–8074
57 Denzer, K., van Eijk, M., Kleijmeer, M. J., Jakobson, E., de Groot, C. and Geuze, H. J. (2000) Follicular dendritic cells carry MHC class II-expressing microvesicles at their surface. J. Immunol. **165**, 1259–1265